Cancer Letters 290 (2010) 192–203

Contents lists available at ScienceDirect

Cancer Letters

journal homepage: www.elsevier.com/locate/canlet

Selective death of human breast cancer cells by lytic immunoliposomes: Correlation with their HER2 expression level

Enrique Barrajón-Catalán [a,1], María P. Menéndez-Gutiérrez [a,1,2], Alberto Falco [a], Alfredo Carrato [b], Miguel Saceda [b], Vicente Micol [a,*]

[a] Molecular and Cellular Biology Institute (IBMC), Miguel Hernández University, Avda. de la Universidad s/n, E-03202 Elche, Alicante, Spain
[b] Elche University Hospital, Biomedical Research Foundation (FIBElx), Camí de la Almazara 11, Ed. Anexo II, 03203 Elche, Alicante, Spain

ARTICLE INFO

Article history:
Received 25 June 2009
Received in revised form 7 September 2009
Accepted 14 September 2009

Keywords:
Trastuzumab
Immunoliposomes
Melittin
Cell lysis
HER2
Anticancer therapy
Breast cancer cells

ABSTRACT

Trastuzumab (Herceptin™) targets the human epidermal growth factor receptor 2 (HER2), which is overexpressed in 20–30% of breast and ovarian cancers carrying a bad prognosis. Our purpose was to target HER2-overexpressing human breast cancer cells with pegylated immunoliposomes bearing trastuzumab and containing melittin, which has recently shown anticancer properties. Using a panel of human breast cancer cells with different HER2 expression levels, these immunoliposomes decreased cancer cells viability in a dose–response manner and in correlation to their level of HER2 expression. Specific binding of the immunoliposomes to SKBr3 breast cancer cells was shown by ImageStream-based analysis. The morphological changes observed in the treated cells suggested a cytolytic process. This preclinical approach may suppose an effective strategy for the treatment of HER2-overexpressing tumors, and can support the development of an early phases I–II clinical trial. Trastuzumab resistant breast cancer cells (JIMT-1), can also be targeted using this approach.

1. Introduction

Nowadays, anticancer chemotherapy obtains incomplete responses and show high toxicity rates because of its side effects on normal cells. Monoclonal antibody (MAb) therapy has contributed to the progress in anticancer therapies results, leading to several clinically approved drugs [1]. The conjugation of complete or fragmented antibodies to liposomes has resulted in the next generation of delivery drugs, i.e., immunoliposomes [2,3]. These provide a targeted drug delivery, enhance selectivity and diminish side effects. In addition, the design of more stable and long-circulating liposomes [4] through their polymeric coating with polyethylene glycol has displayed a retarded clearance by the reticuloendothelial system, prolonging their half life [5]. However, cancer cells have few specific target sites as they share many common features with normal cells. Finding exclusive targets to design selective anticancer drugs is a difficult task.

Abbreviations: HER2/neu HER2, human epidermal growth factor receptor 2; AbDR, lytic immunoliposomes with trastuzumab™; Mab, monoclonal antibody; AMP, antimicrobial peptide; PLA_2, phospholipase 2; EYPC, egg yolk phosphatidylcholine; Chol, cholesterol; DSPE-PEG, 1,2-distearoyl-sn-glycero-3-phosphoethanolamine-PEG-2000; D2000 M, 1,2-distearoyl-sn-glycero-3-phosphoethanolamine-N-[maleimide (PEG 2000)]; DR, lytic liposome (without antibody); Rhod, Lissamine rhodamine dye; Rhod-PE, lissamine rhodamine B 1,2-dihexadecanoyl-sn-glycero-3-phosphoethanolamine; THIS, histidine buffered solution; Rhod-AbDR, rhodamine labeled AbDR; Rhod-DR, rhodamine labeled DR; HPLC, high performance liquid chromatography; AbDR-ø, AbDR immunoliposome without lytic peptide; CC50, concentration corresponding to 50% cytotoxicity; PLD, phospholipase D; DAPI, 4′,6-diamidino-2-phenylindole dye.

* Corresponding author. Tel.: +34 96 6658430; fax: +34 96 6658758.
E-mail address: vmicol@umh.es (V. Micol).

[1] Both authors contributed evenly.

[2] Present address: National Center for Cardiovascular Research Foundation, Regenerative Cardiology Department, C/ Melchor Fernández Almagro, 3, 28029 Madrid, Spain.

0304-3835/$ - see front matter © 2009 Elsevier Ireland Ltd. All rights reserved.
doi:10.1016/j.canlet.2009.09.010

As a promising target, HER2 (or ErbB2) is a protooncogene belonging to the epidermal growth factor receptor family (EGFR or ErbB) of receptor tyrosine kinases (RTK) [6]. HER2 is overexpressed in 20–30% of breast and ovarian cancers [7]. Moreover, in normal adult tissues, HER2 is present only at low levels in certain epithelial cell types [8]. Several anticancer therapies targeting ErbB receptors have been developed, and the humanized monoclonal antibody that binds to HER2 (Herceptin™ or trastuzumab) is currently in clinical use as an effective treatment for HER2 positive breast cancer [9]. Trastuzumab has been used in several therapeutical approaches coupled to liposomes to increase anticancer therapy selectivity. Anti-HER2 immunoliposomes have shown binding and internalization in HER2-overexpressing cells [10], which leads to intracellular drug delivery. Moreover, the use of doxorubicin-loaded anti-HER2 immunoliposomes exhibited significantly higher therapeutic results, in HER2-overexpressing xenograft models, compared to other treatments [11].

Furthermore, antimicrobial peptides (AMPs) are gene encoded natural peptide antibiotics of the innate defenses of many organisms [12]. Several studies have demonstrated that AMPs act on most pathogens, predominantly by disrupting the lipidic cell membranes [13], most probably by forming pores or ion channels [14]. Several models have been proposed to explain this mechanism, i.e., barrel-stave, carpet-like, toroidal pore formation or detergent-type micellization [15], all increasing membrane permeabilization, leakage of cell content and osmotic instability, leading to cell death. In some cases, peptide diffusion to intracellular targets has been also described. The capacity of AMPs to promote cell lysis has been extensively studied in order to develop new anticancer approaches [16].

Among the lytic peptides derived from insects and amphibians, melittin, from bee venom, has recently shown anticancer properties but its precise mechanism of action is still uncertain [17]. Melittin is a 26 aminoacid peptide (GIGAVLKVLTTGLPALISWIKRKRQQ) with α-helix conformation. The primary sequence, due to its particular aminoacid distribution, is the responsible of the amphipathic nature of this peptide: the amino-terminal region (residues 1–20) is predominantly formed by hydrophobic residues whereas the carboxy-terminal region (residues 21–26) is hydrophilic due to the presence of a tandem of basic aminoacids [18].

It has been proposed that the activation of phospholipase A2 (PLA_2) by melittin and the subsequent apoptosis mediated by caspase and metalloproteinases activation is responsible for its activity [19,20]. On the contrary, it is also shown that melittin destroys target membranes by pore formation and destabilization through the barrel-stave mechanism [21,22]. Melittin adsorbs on the cell surface at a low α-helix stage and increases its helicity after insertion into the membrane bilayer leading to pore formation and expansion [21]. Therefore, the mechanism underlying the anticancer activity of melittin remains still unclear.

Recently, pegylated immunoliposomes coupled to a humanized antihepatocarcinoma single-chain antibody variable region fragment were loaded with a bee venom peptide fraction and used to target hepatocarcinoma cells [23]. In the present study, pegylated anti-HER2 immunoliposomes using the complete antibody (trastuzumab) were loaded with melittin and were used against HER2-overexpressing human breast cancer cell lines for the first time. The selective capacity of the immunoliposomes to reduce the viability of several breast cancer cell lines, related to the level of HER2 expression, was determined and compared to the results obtained with the use of the commercial antibody alone. The binding rate of the pharmaceutical preparation has been studied through ImageStream-based analysis in SKBr3 breast cancer cells. The complete characterization of the stability and composition of the immunoliposome preparation was also performed. This immunoliposome system showed efficacy and selectivity against several HER2-overexpressing cancer cell lines.

2. Materials and methods

2.1. Chemicals

1,2-Distearoyl-sn-glycero-3-phosphoethanolamine-N-[maleimide (polyethylene glycol) 2000] (D2000 M) and cholesterol (Chol) were obtained from Avanti Polar Lipids (Birmingham, AL, USA). Lissamine rhodamine B 1,2-dihexadecanoyl-sn-glycero-3-phosphoethanolamine (Rhod-PE) was obtained from Invitrogen (Europe). Natural lipid egg yolk phosphatidylcholine (EYPC) and 1,2-distearoyl-sn-glycero-3-phosphoethanolamine-PEG-2000 (DSPE-PEG) were kindly provided by Lipoid GmbH (Ludwigshafen, Germany). All lipids were dissolved in chloroform/methanol (1:1) and stored at −20 °C. Herceptin™ (trastuzumab) was obtained from ROCHE. DAPI dye was purchased from Molecular Probes (Molecular Probes, Invitrogen, UK). Melittin was purchased from SERVA Electrophoresis (Heidelberg, Germany). Other reagents are described in text.

2.2. Cell lines and cultures

The human breast carcinoma cell lines MCF7 and SKBr3 were obtained from the American Type Culture Collection (ATCC, Manassas, VA). MCF7 breast cancer cells stably overexpressing HER2 oncogene (MCF7/HER2) [24] and the cell line JIMT-1, derived from a breast cancer clinically resistant to trastuzumab [25], both were kindly provided by Institut Català d'Oncologia (Girona, Spain). Cells were routinely grown in DMEM + GlutaMAX medium supplemented with 10% of heat-inactivated fetal bovine serum (GIBCO) and 50 U/mL of penicillin and 50 mg/mL of streptomycin (GIBCO). Cells were incubated at 37 °C in a humified 5% CO_2 air atmosphere.

2.3. Liposome preparation

Liposomes were prepared by lipid film hydration followed by membrane extrusion [26]. Promptly, adequate amounts of each lipid were combined in a molar ratio of 74.5:20:5:0.5 (EYPC:Chol:DSPE-PEG:D2000 M). The organic solvent was evaporated from the lipid solution using a N_2 stream and dried by vacuum for 3 h. The lipid film

was hydrated by vortexing at 25 °C using THIS buffer (1.2 g/L histidine–HCl, 0.78 g/L histidine, pH 7.4). Large unilamellar vesicles were obtained by at least 15× extrusion cycles through 100 nm polycarbonate membranes (Whatman, Maidstone, Kent, UK) using an extruder device (Avestin, Otawa, Canada) [27]. 1% of Rhod-PE was added to the lipid mixture for the flow cytometry assays.

2.4. Antibody derivatization and conjugation to liposomes

The commercial antibody (trastuzumab) was derivatized essentially as previously described [10,28]. Briefly, the antibody was thiolated using 2-iminothiolane (Traut's reagent) and then incubated with the unilamellar vesicles in an Argon inert atmosphere for 12 h at 25 °C with gentle agitation. During the reaction, the thiol group of the derivatized antibody reacted with the maleimide group of the D2000 M lipid present in the liposome yielding the immunoliposome with the antibody covalently attached (the technique is thoroughly reviewed in [29]). When needed, the immunoliposomes were loaded with melittin by incubation with the peptide and maintaining a lipid:peptide ratio of approximately 1:100 for 1 h at 37 °C with gentle agitation, to obtain the final AbDR (antibody-darts) suspension. To eliminate the unbounded antibody and melittin, the mixture was passed through a Sephadex G-25 (Sigma–Aldrich) column using histidine buffer (THIS) buffer for the elution. Isotonic sucrose was added to the melittin-loaded immunoliposome preparations as cryoprotector before lyophilization when these were focused for storage and subsequent reconstitution. Immunoliposome suspensions were lyophilized using a Heto FD2.5 apparatus and stored at 4 °C until utilized. Then, samples were resuspended in distilled water before use.

2.5. Particle size measurements

The size of liposomes was determined by using light scattering technology through intensity measurements, this technique is extensively described in [30,31]. The Zetasizer Nano ZS (Malvern Instruments Ltd., UK) was used to determine the mean vesicle size, size distribution, and polydispersity of the liposomes with the following specifications: 80 s sampling time, 1.33 refractive index, 173° scattering angle and measurement temperature of 25 °C. All the measurements were performed using the AbDR suspension at an approximate concentration of 0.1–0.3 mM. Three independent series of 15–25 individual measurements were obtained for every sample. The typical Nano software DTS version 5.00 was utilized.

2.6. Analytical HPLC

To quantitate the amount of melittin in the immunoliposomes, one volume of methanol was added to the liposome suspension, vortexed and centrifuged. Then, 25 μL were injected in an analytical reverse phase column LiChrospher® 100 RP-18 (5 μm, 250 × 4 mm i.d.) from Merck and subjected to HPLC analysis. The quantitation of melittin was carried out in a high performance liquid chromatography system LaChrom (Merck–Hitachi) series 7000, equipped with a pump, autosampler, column oven and fluorescence detector. The chromatographic analysis was performed at 25 °C and a flow rate of 1.5 mL/min. A mobile phase composed of water:acetonitrile (55:45) and 0.2% trifluoroacetic acid was used under isocratic conditions. Melittin peak was identified by fluorescence detection (absorption at 280 nm and emission at 335 nm) and quantitated by using a melittin standard curve.

2.7. Western blot analysis of HER2 expression

Cells were washed twice with PBS and after scraping them with PBS they were centrifuged at 1500 rpm for 5 min. The cellular pellets were lysed in a lysis buffer containing 50 mM Tris pH 7.4, 1% Igepal CA-630, 150 mM NaCl, 5 mM EDTA and 10 mg/mL of protease inhibitor cocktail (Sigma–Aldrich, Europe). Cells were kept on ice for 20 min and, after a freezing/thawing cycle, they were centrifuged at 12,000 rpm for 5 min. The cellular pellets were discarded and the protein content of the cell extracts (supernatant) was measured by Bradford assay (Bio-Rad, Richmond, CA, USA). Then, 50 μg of protein from each lysate were used for sodium dodecyl sulfate–polyacrylamide gel electrophoresis (SDS–PAGE), transferred to nitrocellulose membranes, incubated with primary monoclonal antibodies against HER2 (sc-284, Santa Cruz Biotechnology, INC) and incubated with horseradish peroxidase-linked secondary antibodies (Sigma–Aldrich, Europe). Proteins were detected by the enhanced chemiluminescence (ECL) method (Amersham International, Buckinghamshire, UK). Densitometric analyses were performed using the SigmaGel gel analysis software (Jandel Scientific, Chicago, IL, USA).

2.8. Quantification of the antibody coupled to the immunoliposomes

Immunoliposome (100 μL) preparation at a lipid concentration of 0.3 mM were concentrated using a SpeedVac Plus SC110A (Savant, Osterville, MA). Then, denaturizing buffer-sample was added prior SDS–PAGE separation. The gels were stained with comassie-blue dying solution for 1 h and decolored with methanol: acetic acid for 2 h. The amount of antibody present in AbDR was quantitated by a semiquantitative method consisting of the comparison between the intensity of HER2 bands deriving from the immunoliposome sample and those of pure antibody (trastuzumab) as standard. The intensity of the bands was quantified by densitometric analysis using a GELPrinter Plus (TDI SA, Spain) and SigmaGel software (Jandel Scientific). Results from liposome stability measurements (size, phospholipid and antibody content) derived from five different liposome preparations.

2.9. Cytotoxicity assay

Cell viability was determined by the MTT assay [32]. Briefly, cells were plated in 96-well plates at a density yielding 80–90% confluence when the cytotoxicity assay was performed. Complete medium was refreshed and six duplicates cultures were treated with different doses of

AbDR for different times. Control samples were treated only with THIS buffer. Viability was then measured by the bioreduction of 3-(4,5-dimethylthiazol-2-yl)-2,5-diphenyltetrazolium-bromide (MTT) to a colored formazan product that was dissolved in 100 μL of DMSO and measured at 570 nm with a microplate reader. The optical density obtained was directly correlated with cell quantity. All the results corresponding to MTT experiments are expressed as the mean of a minimum of 6–8 replicates. Cell viability was alternative measured by crystal violet assay and no significant differences were found compared to MTT assay.

2.10. Flow Cytometry analysis of HER2 expression

MCF7, MCF7/HER2, JIMT-1 and SKBr3 cells were trypsinized and washed repeatedly with PBS-EDTA 0.5% to obtain single cell suspensions. Then, 1.5×10^6 cells of each cell line were fixed in 3.5% Formalin (Sigma–Aldrich Co., St. Louis, MO) during 5 min at 4 °C followed by 10 min at room temperature (RT). After three cycles of washing with PBS-EDTA 0.5%, cells were blocked for 30 min with PBS-BSA 2% at RT. Once the blocking solution was removed, the cells were incubated overnight at 4 °C with gently agitation with a rabbit anti-human HER2/neu antibody (sc-284, Santa Cruz Biotechnology, INC) at a concentration of 0.5 μg/10^5 cells. Cells were washed three times with PBS before proceeding with the secondary antibody staining. Anti-rabbit FITC-conjugated IgG for HER2/neu antibody (F-2765, Molecular Probes) was used as the secondary antibody at a dilution of 1:25 for 30 min at RT. As control, the secondary antibody alone was used after blockade to show nonspecific binding of the IgG to cells. After washing and recollecting cells in PBS, the FITC-stained cells were quantitated by flow cytometry in an Epics XL instrument (Beckman Coulter Co., Miami, Florida) by analyzing the intensity of the green fluorescence associated to cells.

2.11. ImageStream data acquisition and analysis

SKBr3 cells were incubated at 37 °C for 4 h with liposomes labeled with rhodamine-PE, either containing (Rhod-AbDR) or not (Rhod-DR) the anti-HER2 antibody on their surface. Then the cells were trypsinized, washed, recollected at a density of 30×10^6 cells/mL in PBS and directly run on the ImageStream multispectral imaging flow cytometer (Amnis Corporation, Seattle, WA) using 488 nm laser excitation. Classifiers were set when needed to eliminate collection of debris based on low area in the bright-field imagery, clusters of cells based on high area in bright-field imagery, and camera saturating events based on the presence of peak intensities greater than 1022. For all samples imagery excluded by classifiers was observed prior to data collection to ensure that events of interest were not lost. Typical files contained imagery for 5000 cells with each cell imaged with side scatter, bright-field and a channel of fluorescence (rhodamine stain).

Images of cells collected on the ImageStream were analyzed using ImageStream Data Exploration and Analysis Software (IDEAS). The quantitative measurement of liposome cell binding was calculated using features available in IDEAS. The analysis of the fluorescence intensity of rhodamine bound to cells was done in focus-single cells. This classification was performed based on their small bright-field area, high bright-field aspect ratio and high nuclear contrast (as measured by the gradient max feature).

2.12. Microscopy

Images were taken using a Nikon Eclipse TE 2000U fluorescence microscope controlled by NIS-Elements software. DAPI dye, which preferentially stains dsDNA in permeabilized cells, was used following the manufacturer recommendations.

3. Results

3.1. Design and quantitative analysis of anti-HER2 melittin-loaded immunoliposomes

In this study, anti-HER2 coupled immunoliposomes were used to target human breast cancer cells in vitro. For that purpose, large unilamellar vesicles were sterically stabilized by using a pegylated phospholipid. Thereafter, liposomes were covalently coupled through a phospholipidic linker to a commercial anti-HER2 antibody (trastuzumab). Then, purified melittin was added to the immunoliposomes and unbounded peptide was separated through gel chromatography.

All immunoliposome preparations (AbDR) were characterized in size and, also, in lipid, antibody and peptide contents. The lipid concentration was determined by total phosphorus assay [33]. Final melittin:lipid ratio in the liposomes (which was set at 1:100 M theoretical ratio) was determined through the quantitation of melittin by HPLC as described in the Materials section. It showed experimental values around 1:150 ± 10 for freshly prepared liposomes. Size distribution of the immunoliposomes was determined by using light scattering yielding an average size of 139.3 ± 4.7 nm at the day of the preparation with a polydispersity index of 0.127 ± 0.016. The amount of antibody present in the immunoliposomes was quantified as described in the Section 2, and the antibody:liposome ratio was calculated as previously reported [10], showing an average of 32 antibody molecules per liposome (i.e., 29.8 ± 2.7 ng Ab/nmol lipid).

In order to test the stability of the immunoliposome system, all the parameters were evaluated after 5 weeks of storage at 4 °C. There were no drastic changes in the quality of the immunoliposomes. No significant changes were observed neither in size (145.0 ± 6.5 nm) and polydispersity (0.129 ± 0.010, $p < 0.01$), nor in the total antibody amount coupled to the liposomes (27.5 ± 3.4 ng Ab/nmol lipid). However, a decrease in the melittin:lipid ratio was detected after 5 weeks (to 1:700 approximately), probably due to the alteration in the lipid–peptide interactions over the time.

3.2. Expression of HER2 on the breast cancer cell lines

In order to determine the level of HER2/neu expression in the breast cancer cell lines used in this study as a target, western blot analysis was performed on their cell lysates (Fig. 1A). As a control for low or basal expression of HER2 ($\sim 10^4$ receptors/cell), MCF7 cells were used [34]. For positive controls of HER2-overexpressing cell lines ($\sim 10^6$ receptors/cell), SKBr3 and JIMT-1 breast cancer cells were utilized [25,35]. In addition, HER2-overexpressing MCF7 cells (MCF7/HER2) obtained by retroviral transformation were used as positive control [24]. The results derived from western blot analysis showed that SKBr3 and MCF7/HER2 cell lines were highly HER2-positive, whereas the MCF7 cell line was substantially HER2-negative. The expression level of HER2/neu on JIMT-1 cells was also significant compared to MCF7 cells but modest compared to SKBr3 and MCF7/HER2 cells (Fig. 1A).

Since conflicting assessment has been made of the expression of HER2/neu on MCF7 cells [36], the level of expression of HER2 in all the cell lines was unequivocally determined by using flow cytometry analysis (Fig. 1B). Therefore, breast cancer cell lines were phenotyped for surface expression of HER2/neu by flow cytometry. As seen in Fig. 1B, all targets

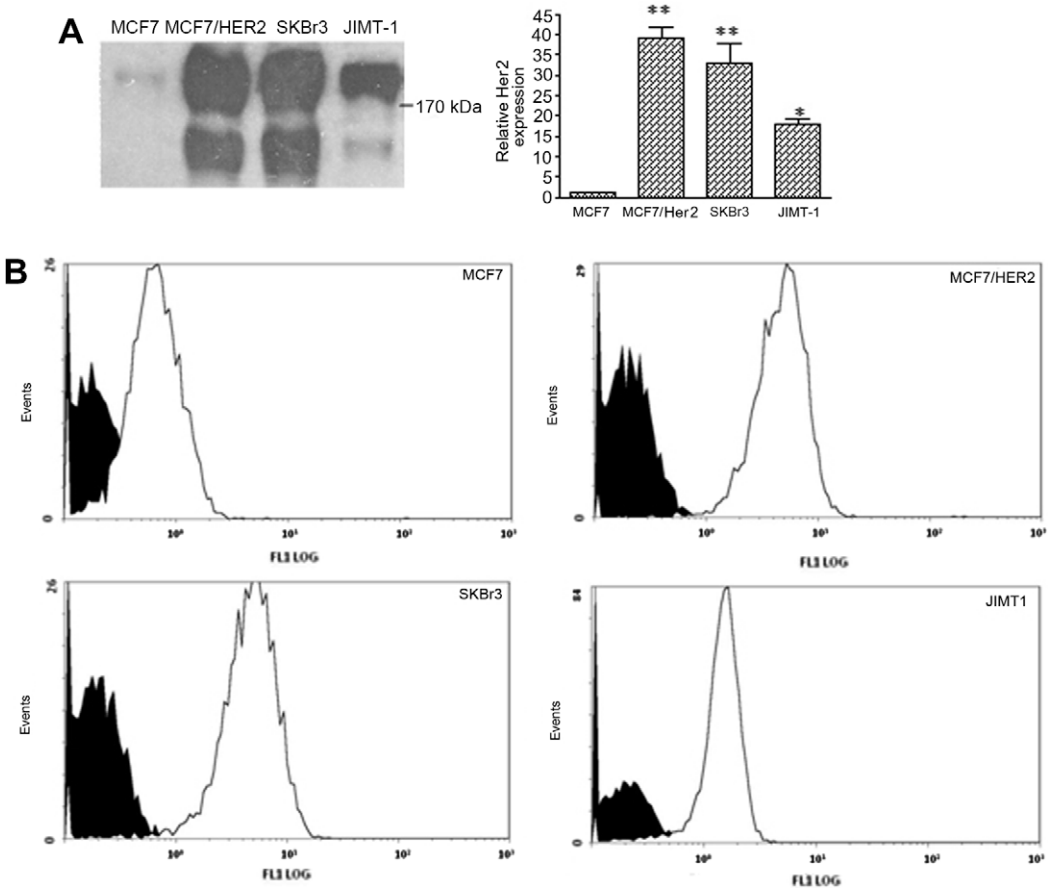

Fig. 1. (A) HER2/neu expression level on breast cancer cell lines determined by western blot analysis and relative HER2 expression quantitation on whole extracts deriving from MCF7, MCF7/HER2, SKBr3 and JIMT-1 cells. Asterisks represent significant differences relative to MCF7 cells ($^{*}p < 0.05$, $^{**}p < 0.01$) ($n = 3$). (B) HER2/neu expression level on same cell lines as Fig. 1A determined by Flow cytometry analysis on cells stained with an anti-HER2/neu antibody. Filled peaks of each histogram represent control cells stained only with the secondary antibody (anti-rabbit-FITC).

were positive for HER2/neu with variable expression. There was a modest binding of anti-HER2/neu IgG to MCF7 cells, whereas there was a significant binding of this antibody to SKBr3 and MCF7/HER2 cell lines. As expected, the level of anti-HER2/neu IgG binding to JIMT-1 cells was intermediate between MCF7 and the HER2/neu overexpressing cell lines, i.e., MCF7/HER2 and SKBr3, which showed similar HER2 expression level.

3.3. Viability of breast cancer cell lines under long-term treatment with trastuzumab

Trastuzumab is clinically approved for the treatment of HER2-overexpressing breast cancer patients. Clinical trials in humans have found through concentrations of ~20 μg/mL trastuzumab and peak plasma concentrations of 185 μg/mL [37]. Moreover, it has been previously reported that 100 μg/mL trastuzumab is a concentration at which HER2/neu overexpressing cells are strongly impaired in their metabolic status [38]. Therefore, we determined the effect of trastuzumab in long-term treatments of 4 days. For these experiments a concentration range of the drug starting at very low levels (compared to clinical data) such as 0.5 μg/mL was utilized. Trastuzumab concentration was raised up to 100 μg/mL in all the breast cancer cell lines studied (Fig. 2). SKBr3 cells were significantly sensitive to the growth inhibitory effects of trastuzumab in a dose dependent manner in agreement to what has been previously reported [39]. Approximately 40% decrease of viability was observed after 4 days of treatment at the highest concentration utilized of trastuzumab, i.e., 100 μg/mL ($p < 0.01$ respect to the rest of cell lines). The growth of these cells was already inhibited at a concentration of trastuzumab as low as 5 μg/mL ($p < 0.01$). Nevertheless, neither MCF7/HER2 cells nor JIMT-1 (both cell lines overexpressing HER2/neu) were affected by the long-term treatment with trastuzumab (Fig. 2). Moreover, the growth of MCF7 cells (with low basal HER2 expression) was not affected by the treatment with the drug either. These results show that viability of breast cancer cell lines treated with trastuzumab seemed to be independent of their HER2 expression level.

3.4. Cytotoxicity studies

Previous results confirmed the low efficacy of trastuzumab to inhibit the growth of breast cancer cell lines with different HER2 expression. Then, immunoliposomes (AbDR) engineered to bear trastuzumab covalently attached to their surface and loaded with a 1:100 melittin:phospholipid ratio were used against the same panel of cell lines. For that purpose, cells were incubated in the presence of increasing concentrations of AbDR and the cytotoxic effect was determined throughout 24 h (Fig. 3A). The results showed that viability of MCF7 cells (with low HER2 expression) was the least affected by the incubation in the presence of AbDR. JIMT-1 cells viability was decreased in a higher degree than that one observed for MCF7 cells. Besides, MCF7/HER2 and SKBr3 cells, which showed the highest levels of HER2 expression, underwent a sharp decrease of their viability at almost all the concentrations of the immunoliposome preparation studied. Therefore, the more expressed HER2 was, the more active AbDR immunoliposome system against the cell line was (Fig. 3A). It can be assumed that high concentrations of immunoliposomes would make the cytotoxic activity to be less cell-specific, since the liposomes have higher probability to reach their targets more easily.

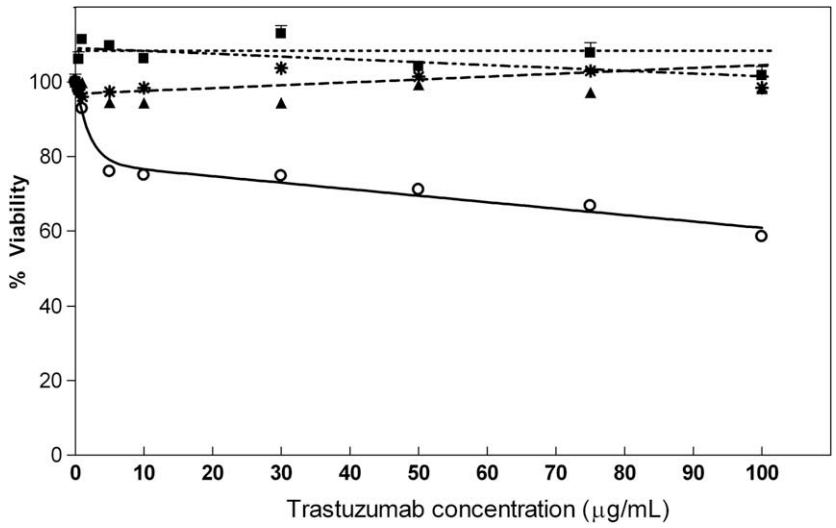

Fig. 2. Cell viability of several breast cancer cell lines (·–·∗ JIMT-1, —▲ MCF7/HER2, –○ SKBr3, - - -■ MCF7) as determined by MTT assay after 4 days of treatment with trastuzumab at concentrations ranging from 0.5 to 100 μg/mL.

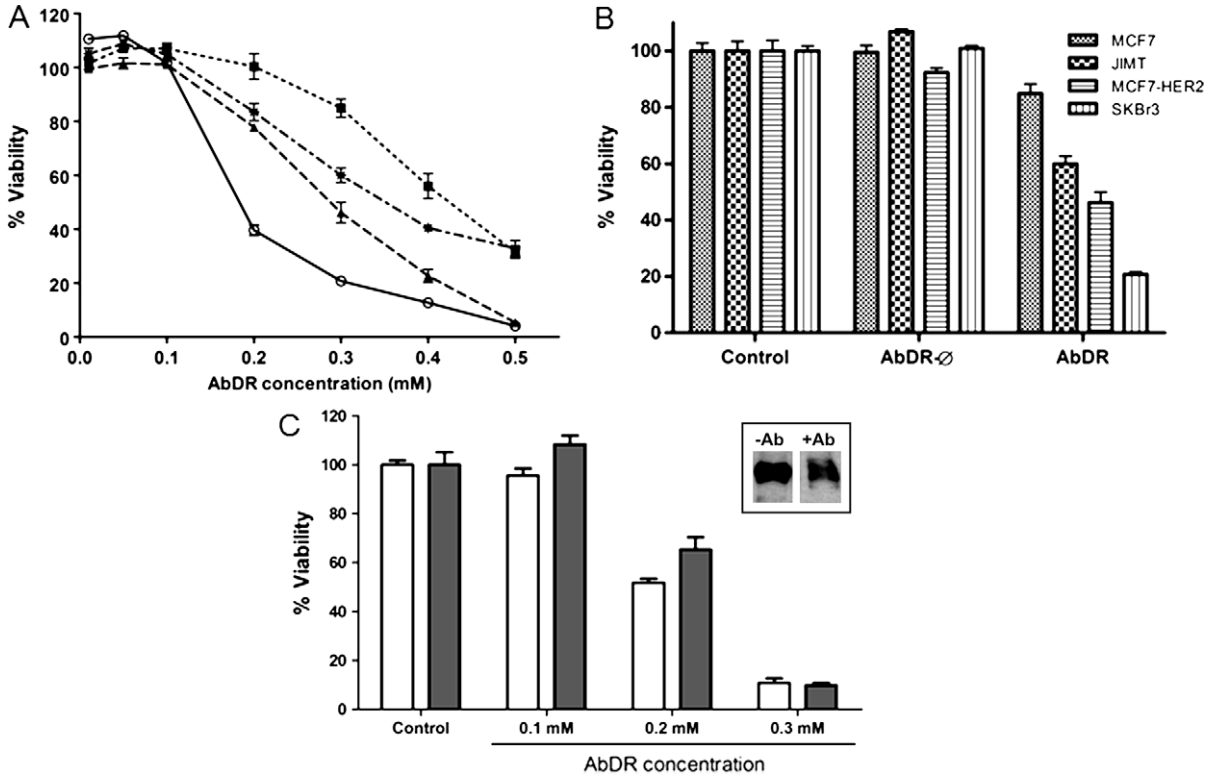

Fig. 3. (A) Plots showing the percentage of viable cells in each breast cancer cell line as determined by MTT assay after 24 h of treatment with AbDR immunoliposomes (·–·∗ JIMT-1, —▲ MCF7/HER2, –○ SKBr3, - - -■ MCF7). Concentration in mM (total phospholipid concentration) is shown in abscise axis. (B) Percentage of viable cells determined by MTT assay for the four breast cancer cell lines after the treatment with 0.3 mM of immunoliposomes coupled to trastuzumab (AbDR-ø) compared to melittin-loaded immunoliposomes coupled to trastuzumab (AbDR) for 24 h (control was THIS buffer). (C) Percentage of viable SKBr3 cells after pretreatment with free trastuzumab at 10 μg/mL for 72 h and the subsequent treatment with AbDR immunoliposomes at the concentrations indicated for 24 h more (grey bars). White bars correspond to non-pretreated cells. Insert shows the anti-HER2 western blot of untreated cells (−Ab), and cells after 72 h of pretreatment with trastuzumab (+Ab).

In order to test the selectivity of the immunoliposome system, immunoliposomes covalently attached to trastuzumab but lacking the peptide (AbDR-ø) were used against the same cell lines in control experiments (Fig. 3B). The concentration of immunoliposomes at which maximum differences between the viability of each cell line were observed, (i.e., 0.3 mM, as seen in Fig. 3A) was selected for that experiment. AbDR-ø

immunoliposomes had almost no effect on the viability of all cell lines at the concentration of 0.3 mM. On the contrary, AbDR immunoliposomes drastically affected the viability of the same cell lines when melittin was present, effect which almost correlated to their HER2 expression level (Fig. 3B).

The exposure of HER2 overexpresssing breast cancer cells to trastuzumab downregulates HER2 expression, diminishing the amount of HER2 protein presented on cell membrane surface [40]. Then, this fact would reduce the cytotoxicity of the AbDR over trastuzumab-pretreated cells, confirming the selectivity of the therapy and rejecting any epiphenomenal influence. To verify this hypothesis, SKBr3 cells were pretreated with 10 μg/mL of trastuzumab for 72 h, which is documented to reduce the HER2 protein levels in the plasmatic membrane around 20–30% [24]. The treatment drastically reduced the level of HER2 expression as seen by western blot analysis (Fig. 3C, insert). Then, cells were treated with different concentrations of the AbDR (0.1–0.3 mM). There were no significant differences at the highest and the lowest concentrations of AbDR tested, on the viability of cells pretreated with trastuzumab compared to those non-treated with the antibody. Nevertheless, when using 0.2 mM of AbDR, the survival of those cells pretreated with trastuzumab (grey bars) was significantly higher than that one of the non-pretreated cells with the antibody (white bars) in correlation to their lower level of HER2 expression (Fig. 3C).

3.5. Efficacy and selectivity of AbDR immunoliposomes upon storage or lyophilization

In order to test the stability of the immunoliposome system, these were stored for 5 weeks at 4 °C after synthesized, and checked for their capacity to decrease cell viability of HER2-overexpressing cell lines every week. After 1 week of storage at 4 °C the immunoliposomes were able to affect cell viability in the same level as in Fig. 3A (data not shown). Measurements performed at the 3rd week on the efficacy of the AbDR on the tested cell lines did not show significant differences regardless the level of HER2 expression of the cell line. However, although AbDR diminished the viability of all the cell lines in a significant way, there was a sharp decrease of selectivity against all the HER2-overexpressing cells what was found around the 3rd week of storage. Stability measurements showed that size and antibody content did not change during storage time, therefore the decrease in selectivity could probably be due to a denaturation phenomenon of trastuzumab, which might be responsible of the unspecific lysis observed in all cell lines. The antibody seemed to be also quite stable when attached to the immunoliposomes upon storage at +4 °C for several days. This fact lead to think that liposome coupling might confer additional stability to trastuzumab. Although the manufacturer claims a shelf life of 48 h for the antibody, almost full activity and selectivity of the immunoliposome system (AbDR) was detected until the 3rd week after synthesis.

As an alternative for 4 °C storage, lyophilization was studied like a preservation method for the immunoliposomes. Different polysaccharides as sucrose, fructose and glucose were tested as cryoprotectors before lyophilization [41] (data not shown). Finally, isotonic sucrose (9.25% w/v) was selected as the best performing one. The immunoliposomes were lyophilized and stored at −20 °C until utilization. AbDR were resuspended in distilled water and then characterized in comparison with freshly prepared AbDR. No changes in size, polydispersity or antibody and melittin levels were found comparing the lyophilized and the freshly synthesized immunoliposome preparations. However, further studies must be performed to check the long-term stability, activity and selectivity of the lyophilized liposomes compared with the 4 °C storage condition.

3.6. Quantitative assessment of AbDR binding and uptake in SKBr3 cells

The novel ImageStream-based analysis employs flow cytometry combined with microscopy and allows for statistical analysis of a variety of cellular parameters as well as the visualization of cells in suspension during flow analysis via high-resolution bright-field, darkfield and fluorescence images [42]. For this purpose, the SKBr3 breast cancer cell line was selected due to its higher response to the immunoliposome treatment. Then, the relative levels of the immunoliposome binding to SKBr3 cells based on the fluorescence of the probe rhodamine were evaluated. This probe was incorporated into immunoliposomes bearing or not the antibody (named Rhod-AbDR and Rhod-DR, respectively) and the rhodamine fluorescence associated to cells was evaluated after the cells were treated with these immunoliposomes. This assay was carried out in SKBr3 cells, in an attempt to verify that the incorporation of trastuzumab antibody to the liposome surface would increase the binding rate of liposome to cells overexpressing the HER2/neu antigen. By employing the ImageStream analysis software (IDEAS), the relative rate of liposome incorporation to SKBr3 cells was determined and compared between Rhod-DR and Rhod-AbDR incubated cells (Fig. 4). Single cells were gated by graphing the mask-corrected parameters of aspect ratio and area. Aggregated cells and debris were not included in further analyses. Cells treated with Rhod-AbDR exhibited a greater amount of debris or non-cellular structures (red signal) than those cells treated with Rhod-DR (Fig. 4A). It has to be considered that after the incubation with Rhod-AbDR, cellular mortality already appeared, so some signals from cellular debris (red signals) may derive from cells which were previously attached to Rhod-AbDR. Therefore, it can be assumed that signal of the Rhod-AbDR-bound cells might be underestimated and the differences compared to Rhod-DR could be even higher. Fig. 4B shows the frequency vs. intensity plots of the cell populations and an image gallery of representative examples of sorted Rhod-DR and Rhod-AbDR subpopulation cells. For quantitation purposes, cell populations were separated in three different groups (A, B, and C) attending to increasing fluorescence intensity signal. Rhod-AbDR treated cells showed higher intensity fluorescence than that one of the Rhod-DR treated cells, which demonstrates the higher specificity of Rhod-AbDR for SKBr3 cells. Fig. 4B shows that Rhod-DR and Rhod-AbDR treated cells evidenced similar A subpopulations (those cells having lowest intensity and Rhod labeling). In contrast, Rhod-AbDR treated cells showed a greater B cell subpopulation than Rhod-DR treated cells (around double, i.e., 28% vs. 14%). Moreover, Rhod-AbDR treated cells showed another cell subpopulation, which supposed 5% of total cells (C), bearing a very strong Rhod labeling intensity, which was negligible in Rhod-DR treated cells. The images corresponding to examples of sorted cells deriving from both treatments (Fig. 4B) clearly showed that B and C subpopulations exhibited a strong rhodamine labeling signal, whereas that one of A subpopulation was almost irrelevant. Considering the percentage of cells and their fluorescence intensity in B and C cell subpopulations, the fluorescence in Rhod-AbDR treated cells was approximately three times higher than that of Rhod-DR treated cells.

3.7. Effects of AbDR on the morphological features of HER2-overexpressing MCF7/HER2 cells

The effect of the AbDR immunoliposomes on the breast cancer cell viability presented here was fairly fast. Microscopy images were taken during a treatment of MCF7/HER2 cells with 0.2 mM of AbDR in order to provide some insight regarding the possible mechanism of cell death. A time-course follow-up of the process was performed during 4 h (Fig. 5), by taking images every minute using a Nikon Eclipse TE 2000U fluorescence microscope and NIS-Elements like the controlling software. The recorded video (see Supporting information) clearly shows that cells died in a few hours suffering a presumably lytic process. In Fig. 5 some pictures extracted from the experiment are shown. As judging from the images, at 1 h treatment (Fig. 5B), a significant number of cells already started to detach from the plate, their cell membrane retracted and became round-shaped. At 2 h treatment (Fig. 5C), most nuclei presented chromatin increasingly granular as the process proceeds and cell membranes continued retracting. At 4 h, cytoplasm of the majority of the cells was almost disintegrated and no viable cells were visible (Fig. 5D). In fact, the video corresponding to this experiment clearly showed a membrane cell disruption process leading to the release of the intracellular content followed by cell membrane retraction.

The lytic effect seemed to be quite fast, occurring in approximately 1–3 h depending on the HER2 expression on the cell line. In order to study more deeply cell morphology, MCF7–HER2 cells were treated with AbDR for 2 h and then DAPI dye, which stains dsDNA in permeabilized cells, was added to the medium to check the integrity of the nucleus (Fig. 6A and B). Apparently, no signs of the formation of apoptotic bodies in the cells were found. It has to be considered that the immunoliposome treatment shown in pictures of Fig. 5A-D corresponds to a cell confluence of only 40%, therefore a more drastic effect on cell viability was observed at 0.2 mM AbDR concentration compared to that one observed in Fig. 3.

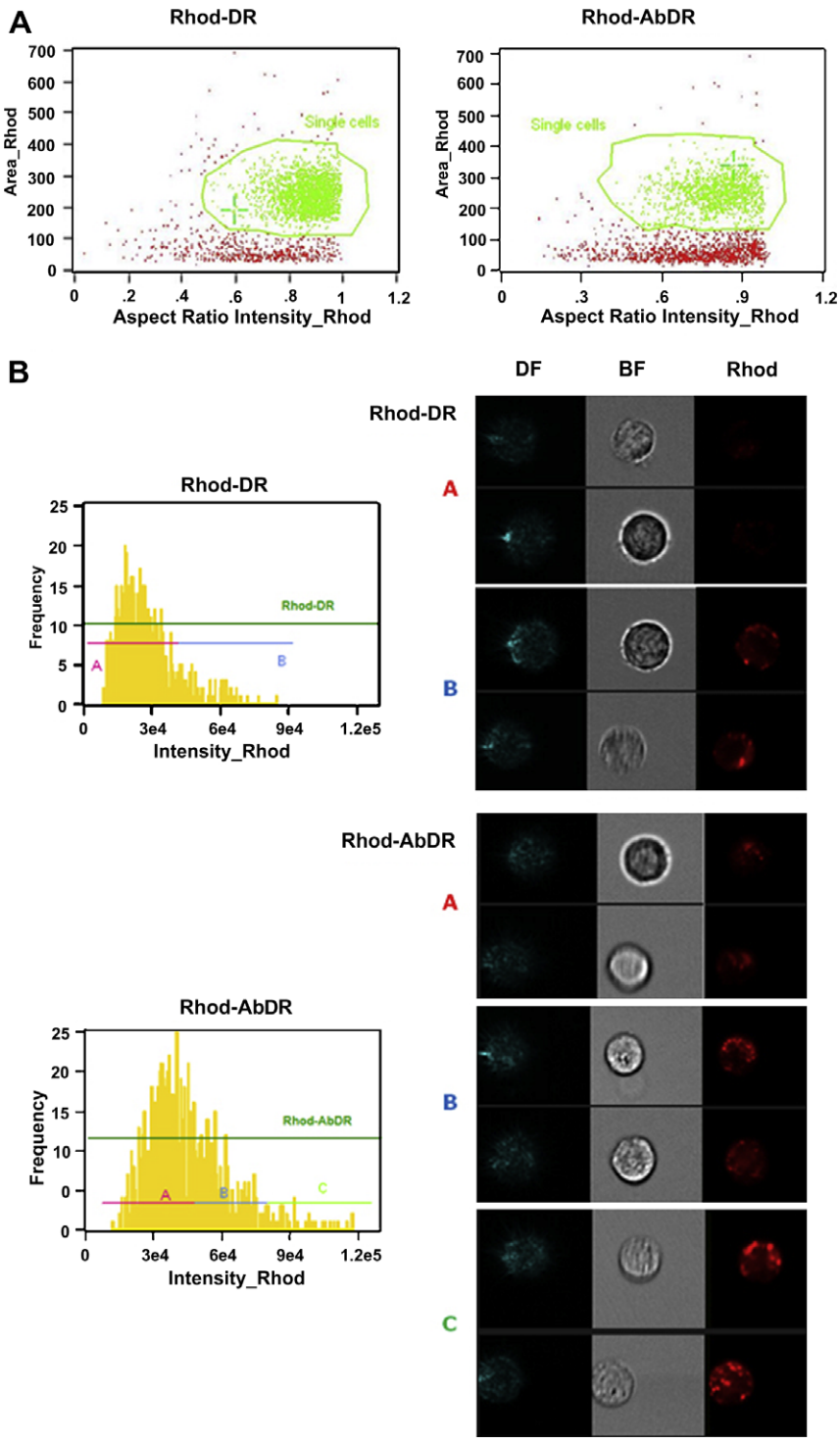

Fig. 4. Quantification of liposome binding to SKBr3 cells treated with Rhod-DR and Rhod-AbDR 0.2 mM for 4 h. **(A)** Plots of area vs. aspect ratio of cells after the incubation with the immunoliposomes. **(B)** Frequency vs. intensity plots of the different cell subpopulations. A, B, and C mean cell subpopulations having increasing fluorescence intensity signal derived from Rhod labeling. The percentages and the intensity mean of rhodamine fluorescence associated to cells are displayed in the histograms. ImageStream fluorescence imaging of sorted A, B and C subpopulations of SKBr3 cells, either treated with Rhod-DR or with Rhod-AbDrR, are shown as composite images of darkfield (DF), bright-field (BF) and rhodamine fluorescence (Rhod).

4. Discussion

In this study, immunoliposomes coupled to a commercial anti-HER2 antibody (trastuzumab) and loaded with melittin, were used for the first time to target breast cancer cell lines which overexpress HER2 receptor. For that purpose, the complete anti-HER2 antibody was used, which has been utilized in previous studies to successfully target HER2-overexpressing cancer cells [43,44].

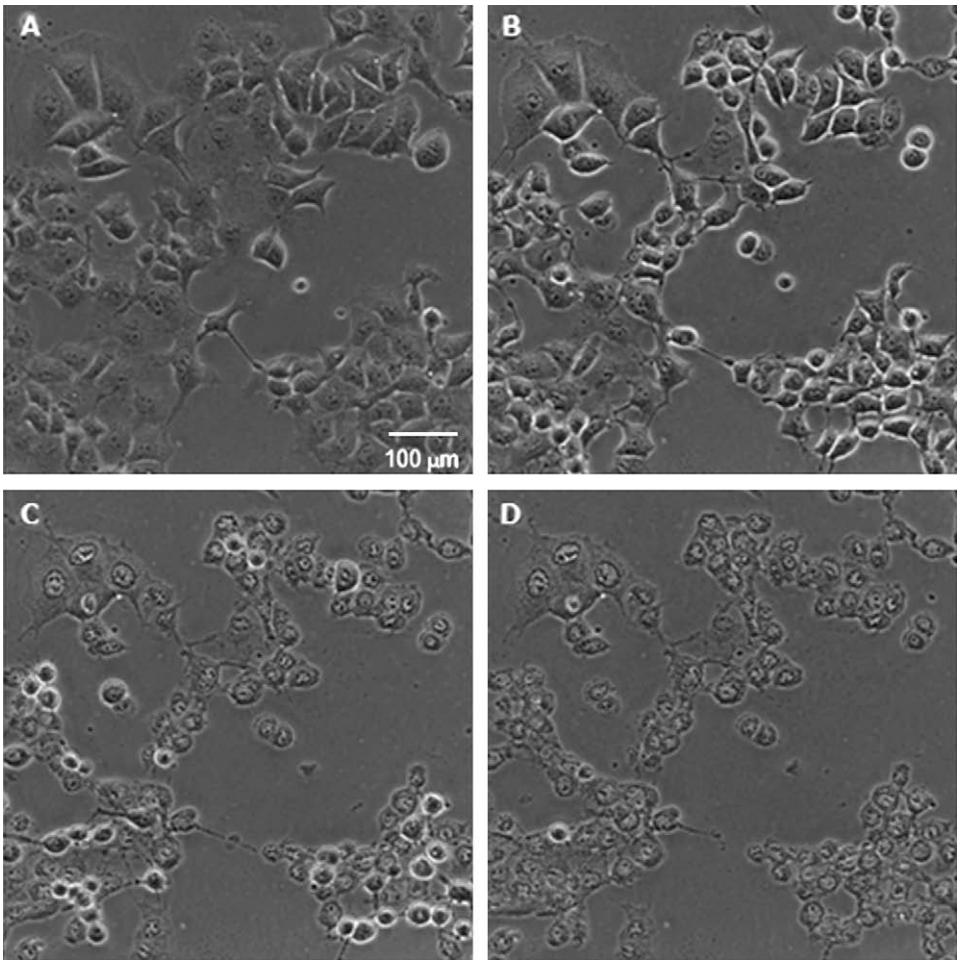

Fig. 5. Images extracted from a time-course follow up experiment of the treatment of MCF7/HER2 cells for 4 h with 0.2 mM of AbDR in a Nikon Eclipse TE 2000U fluorescence microscope. The images were taken a 0 **(A)**, 1 **(B)**, 2 **(C)**, and 4 h **(D)** using a 20× lens.

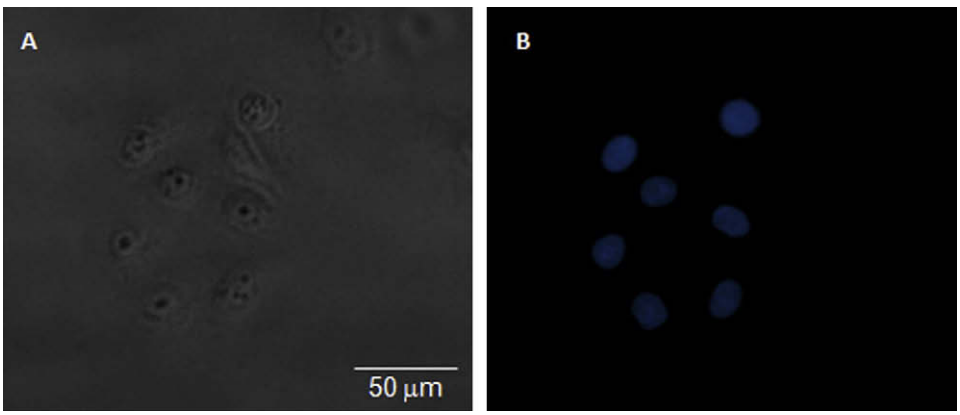

Fig. 6. Contrast phase **(A)** and fluorescence images **(B)** of DAPI staining of MCF7–HER2 cells treated with 0.2 mM AbDR for 2 h, images were taken using 40× lens.

The majority of lytic peptides from insects and amphibians, such as melittin, exhibit a cationic character and display a preference for negatively charged cell membranes or membranes having large membrane potential such as membranes of cancer cells [45], rather than normal cells. Lytic peptides conjugated with hormone segments have been used in order to increase their efficacy and selectivity on several types of cancer cells [46,47]. Nevertheless, a therapy based on this approach might be valid only for those tumors expressing hormone receptors such as prostate or breast cancers. Previous attempts to target cancer cells have been made with melittin-containing immunoliposomes coupled to humanized antihepatoma variable region fragment [23]. Nevertheless no correlation between the liposomes cytotoxic effect and the level of the expression of the target was demonstrated.

The results of the present study show that immunoliposomes (AbDR) drastically decreased the viability of the studied cell lines, which directly correlated to their level of HER2 expression. Maximum efficacy was achieved against MCF7/HER2 and SKBr3 cells, which were those one exhibiting the higher levels of HER2 expression on cell surface, as proven by western blot and flow cytometry analysis. Moreover this effect was confirmed in the same cellular type, i.e., SKBr3, by modulating its HER2 expression level under long-term exposure to trastuzumab. SKBr3 cancer cells treatment with 100 μg/mL of free trastuzumab during 4 days (Fig. 2) was able to reduce their viability in 40%. Equivalent levels of viability reduction were achieved by using as low as 4.87 μg/mL of trastuzumab incorporated onto the immunoliposomes in the same cellular type but in only 24 h. Regardless the length of the treatment, this would indicate that the immunoliposomes therapy showed 20-fold higher efficacy compared to the free antibody.

The efficacy of the immunoliposome system was also compared to that of free trastuzumab in long-term incubations of HER2-overexpressing cancer cell lines. No visible effects on cell viability were observed in MCF7 (with basal HER2 expression), MCF7/HER2 and JIMT-1 (both HER2-overexpressing cell lines) when trastuzumab was used at a high concentration (100 μg/mL) in 4-days treatments. Only SKBr3 cells viability was decreased when cultured in the presence of trastuzumab >5 μg/mL for a long-term period. The specificity of the therapy was also confirmed since all cells treated for 24 h with the immunoliposome system, which contained trastuzumab on their surface and lacking melittin, at a concentration of 0.3 mM (phospholipid) were not affected in their viability. The same concentration of melittin-containing immunoliposomes caused a significant decrease of the cell viability in all the cell lines tested. Furthermore, JIMT-1 breast cancer cells, which have shown to be insensitive to trastuzumab both in vitro and in xenograft tumors [25], could be efficiently targeted and treated using the immunoliposomes, and their cytotoxicity was shown in a short period of time. These results, taken together, confirm the specificity of the immunoliposome system.

In relation to the cytotoxic effects of melittin, striking efficacy differences were observed in our study between free melittin and the immunoliposome system bearing melittin. Anti-HER2 immunoliposomes loaded with melittin started to have a significant effect on HER2-overexpressing breast cancer cells (SKBr3) at concentrations of phospholipid >100 μM, that is around 0.7 μM melittin, and caused almost total cellular destruction at 300 μM phospholipid concentration (i.e., 2 μM melittin). SKBr3 viability curve (Fig. 3A) revealed a CC50 value of 167 ± 7 μM phospholipid concentration which corresponds to a melittin concentration of 1.09 μM. In contrast, free melittin exhibited a CC50 value of 4.12 ± 0.10 μM in the same cell type, what means that the incorporation of melittin into the immunoliposome system increased its cytotoxic efficacy in about four times and provided with selectivity. The calculated CC50 values for the treatments using AbDR in JIMT-1, MCF7/HER2 and MCF7 cells were 277 ± 40 μM, 312 ± 41 μM, and 412 ± 114 μM, respectively.

The analysis of the specific binding of the immunoliposomes to the SKBr3 HER2-overexpressing cells was performed through the use of the novel ImageStream technique, which is more powerful than regular flow cytometry. This technique allows applying statistical analysis to specific cell populations by combining flow cytometry and visualization of cells in suspension during flow analysis. The ImageStream experiments showed that Rhod-AbDR bearing trastuzumab exhibited a much higher level of binding (about three times) to SKBr3 HER2-overexpressing cell line than the same liposomes lacking the antibody (Rhod-DR), as seen by fluorescence labeling using rhodamine. Considering that this technique selects only viable cells and that many cells treated with Rhod-AbDR could be already dead at the time of the measurement (estimated mortality of 30–40% at 0.2 mM AbDR and 4 h treatment), the differences in cell binding of Rhod-AbDR compared to Rhod-DR could be even higher.

Melittin and other peptides from venom of animals have shown anticancer activity [16,17]. Nevertheless, controversial information has emerged in relation to the mechanism underneath the biological activity of melittin. It has been reported that melittin causes apoptosis in cancer cells through the increase of intracellular Ca^{2+} [48], or through the activation of caspases [20], metalloproteinases [19], or cytosolic PLA_2 [49]. On the contrary, other studies propose fast cytolysis or membrane disruption by melittin, i.e., 10–15 min, with the concomitant endogenous phospholipase D (PLD) activation [50].

The cellular effects observed in the present study with the use of melittin-loaded immunoliposomes occurred in a very short time period. Our results lead us to think that cell death of the breast cancer cells takes place through a lytic mechanism more than a caspase-activated apoptosis process. This assumption is in agreement to the membrane disruption process proposed by other authors [50]. Caspase-activated apoptosis triggered by TNF-alpha or radiation in an in vitro system needs at least 12–24 h to show visible cellular events such as DNA fragmentation [51]. Since the effects observed in the presence of AbDR were so fast, the apoptotic pathway should be discarded. The typical features of the apoptotic pathway such as chromatin condensation, membrane blebbing or apoptotic bodies formation [52], were not detected by microscopy in MCF7/HER2 cells treated with the immunoliposomes sys-

tem. In addition, the time-course follow-up microscopy observation of cells at very early stages of the treatment showed outbursts on the cellular membrane what may point to the leakage of cytoplasmic material due to pore formation and subsequent cellular lysis. Hence, the decreases on cell population observed throughout this work in the MTT assays must be attributed to cell death rather than a decrease on cell proliferation.

Therefore, we postulate that melittin rapidly induces cell death in HER2-overexpressing breast cancer cells through the formation of transmembrane pores, probably following the barrel-stavel model [15,21,22]. However, it cannot be discarded that melittin may have additional effects on cancer cells besides its membranolytic effect at lower concentrations and longer-term treatments.

The cytotoxic effects of melittin might be also facilitated upon its incorporation into liposomes. Free melittin in solution establishes an equilibrium between the monomer and tetramer forms due to the electrostatic repulsions of its positive charges [14]. In contrast, the configuration of melittin in the membrane depends on membrane composition and physical properties [15], and encompasses the increase of melittin helicity and aggregation in multimeric forms [22]. Tumor cell membranes contain 3–7 times more phosphatidylserine, a negatively charged phospholipid [45], than normal cells, which may facilitate the insertion of a cationic α-helical peptides such as melittin. In addition, membrane fluidity seems to be also higher in cancer cells, what may also promote pore formation and expansion [22] and, therefore, membrane destabilization.

The immunoliposome system held intact its main features, such as liposome size, coupled antibody and melittin content, throughout 2 weeks following the synthesis. However, lyophilization in isotonic sucrose after synthesis resulted in an appropriate approach for long-term storage of the immunoliposomes. Another advantage of the approach utilized here, compared to immunoliposomes containing chemotherapeutic drugs, is the low toxicity of melittin. Previous studies have demonstrated the absence of side effects on the general physiological functions of rodents at a dosage of 5 mg/kg of melittin either subcutaneous or intradermal [53].

In conclusion, HER2-targeted immunoliposomes coupled to trastuzumab (AbDR) exhibited specific cytotoxicity against HER2-overexpressing breast cancer cells, capacity which correlated with the level of HER2 expression at the cell membranes. Either trastuzumab alone, immunoliposomes lacking melittin or melittin alone were incapable to exhibit such activity. AbDR showed a much higher level of binding to HER2-overexpressing SKBr3 cells as seen by ImageStream technique compared to liposomes lacking antibody. The drastic morphological changes observed through bright-field microscopy suggest a very fast mechanism of cell death starting in less than 1 h after starting the cells' treatment, which might takes place primarily through membrane pore formation. The approach presented here may suppose a specific and effective strategy for the treatment of tumors showing the overexpression of a surface antigen, by using a low toxicity peptide such as melittin. Trastuzumab resistant breast cancer cells (JIMT-1), can be also targeted using this approach. The feasibility of the approach presented here was extended using melittin-loaded immunoliposomes coupled to anti-EpCAM as alternative antibody in a cellular model composed of MCF7 and similar results of efficacy and selectivity were obtained (data not shown).

Conflict of interest

There is no relevant conflict of interest.

Acknowledgments

This investigation has been supported by Grant AGL2007-60778 and private funds provided by CGB-EDSON. We thank personnel of Elche University *Hospital* for their advice and help in the ImageStream analysis and for providing us with the commercial antibody. We also thank Dr. José A. Ferragut from IBMC and Dra. Inmaculada Jiménez from Elche University Hospital and Dr. Jose Solla from Alicante University for their invaluable help.

Appendix A. Supplementary material

Supplementary data associated with this article can be found, in the online version, at doi:10.1016/j.canlet.2009.09.010.

References

[1] M. Sznol, J. Holmlund, Antigen-specific agents in development, Semin. Oncol. 24 (1997) 173–186.
[2] C.O. Noble, D.B. Kirpotin, M.E. Hayes, C. Mamot, K. Hong, J.W. Park, C.C. Benz, J.D. Marks, D.C. Drummond, Development of ligand-targeted liposomes for cancer therapy, Expert Opin. Ther. Targets 8 (2004) 335–353.
[3] J.W. Park, K. Hong, D.B. Kirpotin, D. Papahadjopoulos, C.C. Benz, Immunoliposomes for cancer treatment, Adv. Pharmacol. 40 (1997) 399–435.
[4] D.C. Drummond, O. Meyer, K. Hong, D.B. Kirpotin, D. Papahadjopoulos, Optimizing liposomes for delivery of chemotherapeutic agents to solid tumors, Pharmacol. Rev. 51 (1999) 691–743.
[5] D. Papahadjopoulos, T.M. Allen, A. Gabizon, E. Mayhew, K. Matthay, S.K. Huang, K.D. Lee, M.C. Woodle, D.D. Lasic, C. Redemann, Sterically stabilized liposomes: improvements in pharmacokinetics and antitumor therapeutic efficacy, Proc. Natl. Acad. Sci. USA 88 (1991) 11460–11464.
[6] M.A. Olayioye, R.M. Neve, H.A. Lane, N.E. Hynes, The ErbB signaling network: receptor heterodimerization in development and cancer, EMBO J. 19 (2000) 3159–3167.
[7] D.J. Slamon, G.M. Clark, S.G. Wong, W.J. Levin, A. Ullrich, W.L. McGuire, Human breast cancer: correlation of relapse and survival with amplification of the HER-2/neu oncogene, Science 235 (1987) 177–182.
[8] M.F. Press, C. Cordon-Cardo, D.J. Slamon, Expression of the HER-2/neu proto-oncogene in normal human adult and fetal tissues, Oncogene 5 (1990) 953–962.
[9] D.J. Slamon, B. Leyland-Jones, S. Shak, H. Fuchs, V. Paton, A. Bajamonde, T. Fleming, W. Eiermann, J. Wolter, M. Pegram, J. Baselga, L. Norton, Use of chemotherapy plus a monoclonal antibody against HER2 for metastatic breast cancer that overexpresses HER2, New Engl. J. Med. 344 (2001) 783–792.
[10] D. Kirpotin, J.W. Park, K. Hong, S. Zalipsky, W.L. Li, P. Carter, C.C. Benz, D. Papahadjopoulos, Sterically stabilized anti-HER2 immunoliposomes: design and targeting to human breast cancer cells in vitro, Biochemistry 36 (1997) 66–75.
[11] J.W. Park, K. Hong, D.B. Kirpotin, G. Colbern, R. Shalaby, J. Baselga, Y. Shao, U.B. Nielsen, J.D. Marks, D. Moore, D. Papahadjopoulos, C.C. Benz, Anti-HER2 immunoliposomes: enhanced efficacy attributable to targeted delivery, Clin. Cancer Res. 8 (2002) 1172–1181.

[12] A. Patrzykat, S.E. Douglas, Antimicrobial peptides: cooperative approaches to protection, Protein Peptide Lett. 12 (2005) 19–25.
[13] K. Lohner, S.E. Blondelle, Molecular mechanisms of membrane perturbation by antimicrobial peptides and the use of biophysical studies in the design of novel peptide antibiotics, Comb. Chem. High Throughput Screen. 8 (2005) 241–256.
[14] B. Bechinger, Structure and functions of channel-forming peptides: magainins, cecropins, melittin and alamethicin, J. Membrane Biol. 156 (1997) 197–211.
[15] D. Allende, S.A. Simon, T.J. McIntosh, Melittin-induced bilayer leakage depends on lipid material properties: evidence for toroidal pores, Biophys. J. 88 (2005) 1828–1837.
[16] D.W. Hoskin, A. Ramamoorthy, Studies on anticancer activities of antimicrobial peptides, Biochim. Biophys. Acta 1778 (2008) 357–375.
[17] D.J. Son, J.W. Lee, Y.H. Lee, H.S. Song, C.K. Lee, J.T. Hong, Therapeutic application of anti-arthritis, pain-releasing, and anti-cancer effects of bee venom and its constituent compounds, Pharmacol. Ther. 115 (2007) 246–270.
[18] H. Raghuraman, A. Chattopadhyay, Melittin: a membrane-active peptide with diverse functions, Biosci. Rep. 27 (2007) 189–223.
[19] L. Holle, W. Song, E. Holle, Y. Wei, T. Wagner, X. Yu, A matrix metalloproteinase 2 cleavable melittin/avidin conjugate specifically targets tumor cells in vitro and in vivo, Int. J. Oncol. 22 (2003) 93–98.
[20] D.O. Moon, S.Y. Park, M.S. Heo, K.C. Kim, C. Park, W.S. Ko, Y.H. Choi, G.Y. Kim, Key regulators in bee venom-induced apoptosis are Bcl-2 and caspase-3 in human leukemic U937 cells through downregulation of ERK and Akt, Int. Immunopharmacol. 6 (2006) 1796–1807.
[21] S.F. Sui, H. Wu, Y. Guo, K.S. Chen, Conformational changes of melittin upon insertion into phospholipid monolayer and vesicle, J. Biochem. 116 (1994) 482–487.
[22] J.H. Lin, A. Baumgaertner, Stability of a melittin pore in a lipid bilayer: a molecular dynamics study, Biophys. J. 78 (2000) 1714–1724.
[23] H. Hu, D. Chen, Y. Liu, Y. Deng, S. Yang, M. Qiao, J. Zhao, X. Zhao, Target ability and therapy efficacy of immunoliposomes using a humanized antihepatoma disulfide-stabilized Fv fragment on tumor cells, J. Pharm. Sci. 95 (2006) 192–199.
[24] J.A. Menendez, A. Vazquez-Martin, R. Colomer, J. Brunet, A. Carrasco-Pancorbo, R. Garcia-Villalba, A. Fernandez-Gutierrez, A. Segura-Carretero, Olive oil's bitter principle reverses acquired autoresistance to trastuzumab (Herceptin) in HER2-overexpressing breast cancer cells, BMC Cancer 7 (2007) 80.
[25] M. Tanner, A.I. Kapanen, T. Junttila, O. Raheem, S. Grenman, J. Elo, K. Elenius, J. Isola, Characterization of a novel cell line established from a patient with Herceptin-resistant breast cancer, Mol. Cancer. Ther. 3 (2004) 1585–1592.
[26] F. Olson, C.A. Hunt, F.C. Szoka, W.J. Vail, D. Papahadjopoulos, Preparation of liposomes of defined size distribution by extrusion through polycarbonate membranes, Biochim. Biophys. Acta 557 (1979) 9–23.
[27] S. Vemuri, C.T. Rhodes, Preparation and characterization of liposomes as therapeutic delivery systems: a review, Pharm. Acta Helv. 70 (1995) 95–111.
[28] J. Huwyler, D. Wu, W.M. Pardridge, Brain drug delivery of small molecules using immunoliposomes, Proc. Natl. Acad. Sci. USA 93 (1996) 14164–14169.
[29] C.B. Hansen, G.Y. Kao, E.H. Moase, S. Zalipsky, T.M. Allen, Attachment of antibodies to sterically stabilized liposomes: evaluation, comparison and optimization of coupling procedures, Biochim. Biophys. Acta 1239 (1995) 133–144.
[30] Dynamic light scattering: an introduction in 30 min, Malvern Instruments technical note (MRK656-01), Malvern Instruments Ltd., 2008. Available from: <http://www.malvern.com/common/downloads/campaign/MRK656-01.pdf>.
[31] V. Villari, N. Micali, Light scattering as spectroscopic tool for the study of disperse systems useful in pharmaceutical sciences, J. Pharm. Sci. 97 (2008) 1703–1730.
[32] T. Mosmann, Rapid colorimetric assay for cellular growth and survival: application to proliferation and cytotoxicity assays, J. Immunol. Methods 65 (1983) 55–63.
[33] C.H. Fiske, Y. Subbarow, The colorimetric determination of phosphorus, J. Biol. Chem. 66 (1925) 375–400.
[34] G.D. Lewis, I. Figari, B. Fendly, W.L. Wong, P. Carter, C. Gorman, H.M. Shepard, Differential responses of human tumor cell lines to anti-p185HER2 monoclonal antibodies, Cancer. Immunol. Immunother. 37 (1993) 255–263.
[35] P.B. Lam, L.N. Burga, B.P. Wu, E.W. Hofstatter, K.P. Lu, G.M. Wulf, Prolyl isomerase Pin1 is highly expressed in Her2-positive breast cancer and regulates erbB2 protein stability, Mol. Cancer 7 (2008) 91.
[36] S. Cooley, L.J. Burns, T. Repka, J.S. Miller, Natural killer cell cytotoxicity of breast cancer targets is enhanced by two distinct mechanisms of antibody-dependent cellular cytotoxicity against LFA-3 and HER2/neu, Exp. Hematol. 27 (1999) 1533–1541.
[37] M.D. Pegram, A. Lipton, D.F. Hayes, B.L. Weber, J.M. Baselga, D. Tripathy, D. Baly, S.A. Baughman, T. Twaddell, J.A. Glaspy, D.J. Slamon, Phase II study of receptor-enhanced chemosensitivity using recombinant humanized anti-p185HER2/neu monoclonal antibody plus cisplatin in patients with HER2/neu-overexpressing metastatic breast cancer refractory to chemotherapy treatment, J. Clin. Oncol. 16 (1998) 2659–2671.
[38] G.E. Konecny, M.D. Pegram, N. Venkatesan, R. Finn, G. Yang, M. Rahmeh, M. Untch, D.W. Rusnak, G. Spehar, R.J. Mullin, B.R. Keith, T.M. Gilmer, M. Berger, K.C. Podratz, D.J. Slamon, Activity of the dual kinase inhibitor lapatinib (GW572016) against HER-2-overexpressing and trastuzumab-treated breast cancer cells, Cancer Res. 66 (2006) 1630–1639.
[39] S.L. Moulder, F.M. Yakes, S.K. Muthuswamy, R. Bianco, J.F. Simpson, C.L. Arteaga, Epidermal growth factor receptor (HER1) tyrosine kinase inhibitor ZD1839 (Iressa) inhibits HER2/neu (erbB2)-overexpressing breast cancer cells in vitro and in vivo, Cancer Res. 61 (2001) 8887–8895.
[40] J. Baselga, J. Albanell, Mechanism of action of anti-HER2 monoclonal antibodies, Ann. Oncol. 12 (Suppl. 1) (2001) S35–S41.
[41] W.Q. Sun, A.C. Leopold, L.M. Crowe, J.H. Crowe, Stability of dry liposomes in sugar glasses, Biophys. J. 70 (1996) 1769–1776.
[42] E.K. Zuba-Surma, M. Kucia, A. Abdel-Latif, J. Lillard Jr., M.Z. Ratajczak, The ImageStream system: a key step to a new era in imaging, Folia Histochem. Cytobiol. 45 (2007) 279–290.
[43] T. Kikumori, T. Kobayashi, M. Sawaki, T. Imai, Anti-cancer effect of hyperthermia on breast cancer by magnetite nanoparticle-loaded anti-HER2 immunoliposomes, Breast Cancer Res. Treat. 113 (2009) 435–441.
[44] M. Kullberg, K. Mann, J.L. Owens, A two-component drug delivery system using Her-2-targeting thermosensitive liposomes, J. Drug. Target 17 (2009) 98–107.
[45] T. Utsugi, A.J. Schroit, J. Connor, C.D. Bucana, I.J. Fidler, Elevated expression of phosphatidylserine in the outer membrane leaflet of human tumor cells and recognition by activated human blood monocytes, Cancer Res. 51 (1991) 3062–3066.
[46] B. Gawronska, C. Leuschner, F.M. Enright, W. Hansel, Effects of a lytic peptide conjugated to beta HCG on ovarian cancer: studies in vitro and in vivo, Gynecol. Oncol. 85 (2002) 45–52.
[47] W. Hansel, F. Enright, C. Leuschner, Destruction of breast cancers and their metastases by lytic peptide conjugates in vitro and in vivo, Mol. Cell. Endocrinol. 260–262 (2006) 183–189.
[48] S.T. Chu, H.H. Cheng, C.J. Huang, H.C. Chang, C.C. Chi, H.H. Su, S.S. Hsu, J.L. Wang, I.S. Chen, S.I. Liu, Y.C. Lu, J.K. Huang, C.M. Ho, C.R. Jan, Phospholipase A2-independent Ca^{2+} entry and subsequent apoptosis induced by melittin in human MG63 osteosarcoma cells, Life Sci. 80 (2007) 364–369.
[49] A.S. Arora, P.C. de Groen, D.E. Croall, Y. Emori, G.J. Gores, Hepatocellular carcinoma cells resist necrosis during anoxia by preventing phospholipase-mediated calpain activation, J. Cell Physiol. 167 (1996) 434–442.
[50] S.S. Saini, A.K. Chopra, J.W. Peterson, Melittin activates endogenous phospholipase D during cytolysis of human monocytic leukemia cells, Toxicon 37 (1999) 1605–1619.
[51] B. Yan, H. Wang, D. Zhuo, F. Li, T. Kon, M. Dewhirst, C.Y. Li, Apoptotic DNA fragmentation factor maintains chromosome stability in a P53-independent manner, Oncogene 25 (2006) 5370–5376.
[52] A.H. Wyllie, Apoptosis: an overview, Br. Med. Bull. 53 (1997) 451–465.
[53] H.W. Kim, Y.B. Kwon, T.W. Ham, D.H. Roh, S.Y. Yoon, S.Y. Kang, I.S. Yang, H.J. Han, H.J. Lee, A.J. Beitz, J.H. Lee, General pharmacological profiles of bee venom and its water soluble fractions in rodent models, J. Vet. Sci. 5 (2004) 309–318.